The Role of the LH Sub-domain in the Function of the Cip/Kip Cyclin Dependent Kinase Regulators

Steve Otieno[1], Christy R. Grace[1], and Richard W. Kriwacki[1,2*]

[1]Department of Structural Biology, St. Jude Children's Research Hospital, Memphis, TN 38105
[2]Department of Microbiology, Immunology and Biochemistry, The University of Tennessee Health Science Center, Memphis, TN 38163

* Corresponding Author: Tel: +1 901-595-3290; fax 1 901-595-3032.
Email address: richard.kriwacki@stjude.org (R.W. Kriwacki).

Running Title: The Cip/Kip LH Sub-domain

Keywords: p27; cyclin-dependent kinase inhibitors; isothermal titration calorimetry; intrinsically disordered proteins; cell cycle; nuclear magnetic resonance

SUPPORTING MATERIAL

Materials and Methods

Expression and purification of unlabeled proteins and peptides

Oligonucleotides encoding the p21, p27, and p57 sub-domain LH peptides were ligated into a modified pET28a plasmid vector (Novagen, Gibbstown, NJ). The modified pET28a plasmid has tandem GST and His affinity tags upstream of the peptide cloning region such that the peptides were expressed as GST-His fusion proteins. The fusion proteins were expressed in *E. coli* BL21 DE3 (Novagen, Gibbstown, NJ) and purified using Ni^{2+}- and glutathione-affinity chromatography (GE Healthcare, Piscataway, NJ) followed by cleavage of the affinity tags with thrombin (Novagen, Gibbstown, NJ). Thrombin cleavage left four exogenous amino acids, GSHM, at the N-termini of the sub-domain LH peptides. Cleaved peptides were further purified by high-performance liquid chromatography (HPLC) using a C18 column (Vydac, Hesperia, CA) and a water, acetonitrile, 0.1% trifluoroacetic acid solvent system. p27-KID^{wt} was expressed as a His-tagged fusion protein and purified using established procedures (1). DNA encoding p27-KID^{wt} (residues 22-105 of human p27) was ligated into the pET28-GST-His plasmid (pET28-GST-His-p27-KID^{wt}) between NdeI and EcoRI restriction sites. To create expression vectors for the chimeric p27 LH sub-domain variants, oligonucleotides encoding the LH sub-domains of human p21 and p57, and the LH3G mutant sub-domain, were ligated into the pET28-GST-His-p27-KID^{wt} plasmid using cassette mutagenesis. p27-KID^{wt} was expressed as a His-tagged fusion protein and purified using established procedures (1). The LH sub-domain variants (p27-KID^{p21LH}, p27-KID^{p57LH} and p27-KID^{LH3G}) were expressed in *E. coli* and purified using Ni^{2+}-affinity chromatography followed by cleavage of the GST-His tag using thrombin. The cleavage solutions were boiled for 20 minutes (2) and cleared by centrifugation to yield pure p27 variants as determined by by SDS-PAGE. A peptide corresponding to the Cdk-binding sub-domain of p27 (D2; residues 58-105) was expressed as a His-tagged fusion protein and purified using established procedures (1). The p27 cyclin binding domain peptide (D1; residues 25-37) and the $p27^{LH3G}$ LH sub-domain peptide were prepared by solid phase synthesis (Hartwell Center, St. Jude Children's Research Hospital, Memphis, TN). Human cyclin A (residues 173-432) and full length human Cdk2 phosphorylated on threonine 160 were expressed and purified using established procedures (1, 3). The Cdk2/cyclin A complex was prepared by mixing the purified components (1:1 mole ratio), incubation at 4 °C for 30 minutes, and purification using gel filtration chromatography (Superdex 75, GE Healthcare, Piscataway, NJ) using gel filtration buffer (GF buffer; 20 mM HEPES pH 7.5, 300 mM NaCl, 5 mM DTT). The ternary complexes used in the thermal denaturation experiments were prepared by mixing p27-KID^{wt} or p27 LH sub-domain variants with the Cdk2/cyclin A complex in a 1.1:1 mole ratio, incubation at 4 °C for 30 minutes, and purification using gel filtration chromatography (Superdex 200, GE Healthcare, Piscataway, NJ) and GF buffer. Before use in ITC or thermal denaturation experiments, p27-KID^{wt} and the LH sub-domain variants were treated with 100 mM DTT at room temperature for 30 minutes followed by buffer exchange using gel filtration chromatography (Superdex 75, GE Healthcare, Piscataway, NJ) into the ITC buffer (20 mM HEPES pH 7.5, 300 mM NaCl, 5 mM DTT) or the thermal denaturation buffer (1 mM sodium phosphate pH 7.0, 25 mM NaCl and 1 mM DTT), respectively.

Labeling of proteins for NMR

The methyl labeling was achieved by selectively protonating and ^{13}C labeling the methyl groups of isoleucine, leucine and valine residues using 100 mg/L of (3-Methyl-^{13}C, 99%; 3, 4, 4-D_4, 98%) α-Ketoisovaleric acid, and 50 mg/L of (Methyl-^{13}C, 99%; 3, 3 D_2, 98%) α-Ketobutyric acid (Cambridge Isotope Laboratories, Andover, MA). In addition to the methyl labeling reagents, cells were grown in $^{2}H_2O$/MOPS-based minimal media supplemented with $^{15}NH_4Cl$ (4). The methyl labeling reagents were added 1 hour prior to induction with isopropyl-β-D-thiogalactopyranoside (IPTG) and the cells were grown for an additional 4 hours at 37 °C after induction. The proteins were purified as described above for unlabeled p27-KID variants.

Protein concentration determination

Protein concentrations were determined by UV absorbance at 280 nm in a denaturing buffer containing 20 mM sodium phosphate, pH 6.5, and 6.0 M guanidinium hydrochloride (5, 6). The following molar extinction coefficients, determined using the ProteinParameters tool (ExPASy server; http://us.expasy.org/tools/protparam.html), were used for determining protein concentrations: 15,220 M^{-1} cm^{-1} for p27-KID^{wt}, p27-KID^{p57LH} and p27-KID^{LH3G}; 15,470 M^{-1} cm^{-1} for D2 and p27-KID^{p21LH}, and 35,560 M^{-1} cm^{-1}, 31,860 M^{-1} cm^{-1} and 33,710 M^{-1} cm^{-1} for Cdk2, cyclin A, and the Cdk2/cyclin A complex, respectively. The molar extinction coefficient used for the p27-KID^{wt}, p27-KID^{p57LH}, p27-KID^{LH3G} ternary complexes (with Cdk2/cyclin A) was 24,465 M^{-1} cm^{-1} and that used for the p27-KID^{p21LH} ternary complex was 24,590 M^{-1} cm^{-1}. To facilitate concentration determination, the sequences of the peptides corresponding to the LH sub-domains of p21, p27 and p57, that lack aromatic residues which absorb UV light, were each extended to include a tryptophan residue at the C-terminus. A conserved tryptophan residue is found at the N-terminus of sub-domain D2 in p21, p27 and p57; therefore, inclusion of this residue at the C-terminus of the LH sub-domain peptides did not introduce non-natural features. The extinction coefficient used for the p21, p27, and p57 LH sub-domain peptides was 5,690 M^{-1} cm^{-1}. The concentration of the p27^{LH3G} LH sub-domain peptide was determined by amino acid analysis (AAA Service Laboratory, Damascus, OR)

ITC experiments

An initial injection of 2 μl was followed by 39 injections of 6 μl each at 300 second intervals. Samples for ITC experiments were exhaustively dialyzed against ITC buffer (20 mM HEPES pH 7.5, 300 mM NaCl and 5 mM DTT). The protein concentrations for ITC experiments were as follows: 75 μM p27-KID^{wt} + 7.4 μM Cdk2/cyclin A; 73 μM D1 + 5.2 μM Cdk2/cyclin A; 72.3 μM D2 + 5.6 μM Cdk2/cyclin A; 56.9 μM p27-KID^{p21LH} + 6.2 μM Cdk2/cyclin A complex; 53.6 μM p27-KID^{p57LH} + 4.6 μM Cdk2/cyclin A; and 35 μM p27-KID^{LH3G} + 2.9 μM Cdk2/cyclin A. Samples were degassed immediately prior to use and the instrument was regularly calibrated using the manufacturer's procedures. Raw ITC binding data were fit to a 1:1 binding model using an algorithm provided by the manufacturer using Origin software (GE Healthcare, Piscataway, NJ).

Thermal denaturation experiments

The 1:1:1 ternary complex samples (400 nM) dissolved in 1 mM sodium phosphate buffer, pH 7.0, 25 mM NaCl and 1 mM DTT, were analyzed in a 1 cm path length quartz cuvette (Hellma, Plainview, NY). The temperature dependence of denaturation was determined by

monitoring ellipticity at 222 nm measured at 1 °C intervals using a heating rate of 5 °C min^{-1} and equilibration for 1 min at each temperature with constant stirring. The final results represent the average of either duplicate (ternary complexes with p27-KID^{p21LH} and p27-KID^{LH3G}) or triplicate (ternary complexes with p27-KID^{wt} and p27-KID^{p57LH}) measurements. Denaturation curves were analyzed as previously described (3) to derive values of the thermal denaturation temperature (T_m^{app}).

NMR Experiments

The various binary and ternary complex samples were dissolved in buffer composed of 20 mM potassium phosphate pH 6.5, 50 mM arginine, 10% (v/v) ^2H_2O, 5 mM DTT, and 0.02% (w/v) sodium azide each at a concentration of 0.3 mM; spectra were recorded at308 K. The spectra were processed using NMRPipe software (7) and analyzed using the computer-aided resonance software (CARA) (8). For each sample, the [^{1}H,^{15}N] TROSY spectrum was collected with 96 scans with 2048 points for ^{1}H and 128 points for the ^{15}N dimension, with the corresponding spectral widths of 16 and 30 ppm (26.3 msec maximum t_1 evolution time), respectively. The data were zero-filled to 2024 X 1024 points prior to Fourier transformation. The [^{1}H,^{13}C] HMQC spectra were measured with 96 scans with 512 points for ^{1}H and 128 points for the ^{13}C dimensions with the corresponding spectral widths of 6 and 24 ppm (13.4 msec maximum ^{13}C t_1 evolution time), The data were multiplied by 90-shifted sine bell function and zero-filled to 1024 X 1024 points prior to Fourier transformation. Assignments of ^1H_N and $^{15}N_H$ resonances were available (9) and the assignments of ^{1}H, ^{13}C methyl resonances of a sub-set of the Leu and Val residues were obtained through analysis of complexes with different p27-KID constructs bound to Cdk2, cyclin A or Cdk2/cyclin A, as described below.

Assignment of Methyl Resonances

A sub-set of Leu and Val ^{13}C/^{1}H methyl resonances for the p27-KID constructs bound to Cdk2/cyclin A were analyzed to complement the more complete analysis based on backbone HN resonances in 2D [^{1}H,^{15}N] TROSY spectra. The sequence of p27-KID (spanning residues 22-105 of human p27) contains five Leu residues (Leu32, Leu41, Leu45, Leu70, and Leu84) and three Val residues (Val36, Val79 and Val101). Therefore, the 2D [^{1}H,^{13}C] HMQC spectrum of free p27-KID should exhibit 16 methyl resonances in total with random coil chemical shift values [from http://www.bmrb.wisc.edu], as follows. Five pairs of Leu resonances at ~25 ppm/~0.93 ppm (^{13}C/^{1}H) for the δ_1 CH_3 and ~23 ppm/~0.88 ppm for the δ_2 CH_3 and three pairs of Val resonances at ~21 ppm/~0.96 ppm for the γ_1 CH_3 and ~20 ppm/~0.96 ppm for the γ_2 CH_3 (Fig. S3A in the Supporting Material). These methyl resonances for p27-KID have not previously been assigned. For this study, we chose to analyze a small sub-set of these methyl resonances within sub-domains D1 and D2 as reporters of the Cdk2/cyclin A-bound conformation of wild-type p27-KID and the variant LH sub-domain constructs. This strategy was undertaken to confirm that certain Leu and Val residues within the D1 and D2 sub-domains of the different KID constructs bound similarly to cyclin A and Cdk2, respectively, within the ternary complexes with Cdk2/cyclin A. Our strategy for assigning in total four methyl resonances (as conformational reporters) involved the comparison of the 2D [^{1}H,^{13}C] HMQC spectrum for isolated ^{15}N/^{2}H-(I)LV-^{13}C/^{1}H-labeled p27-KID (Fig. S3A in the Supporting Material) and others obtained when p27-KID was bound to cyclin A, Cdk2, sub-domain D2, or Cdk2/cyclin A (Fig. S3B-D, respectively, in the Supporting Material). The pattern of resonances observed in the 2D [^{1}H,^{13}C] HMQC spectrum for p27-KID, which exhibits resonance overlap for

the different types of Leu and Val methyl groups, is consistent with the amino acid sequence and the disordered nature of this polypeptide. It should be noted that, under the conditions of the NMR measurements with ternary complexes, Cdk2/cyclin A unfolds and precipitates over time, releasing some amount of isotope-labeled, free p27-KID. Unfortunately, this process occurred to different extents for the different binary and ternary complexes. Therefore, "extra" peaks for free p27-KID appear at different amplitudes in the 2D [^{1}H,^{13}C] HMQC spectra for binary and ternary complexes.

Counting Leu and Val methyl resonances for the p27-KID/Cdk2/cyclin A complex. Comparison of the spectra for free p27-KID and p27-KID/Cdk2/cyclin A (Fig. S3A and E, respectively, in the Supporting Material) reveals 14 resonances that exhibit chemical shifts different from those associated with free p27-KID. These resonances arise from five Leu and two Val residues within the KID that fold upon binding Cdk2/cyclin A. Val101 remains disordered when the KID is bound to Cdk2/cyclin A (1, 10) and, therefore, the resonances for this residue are overlapped with the free p27-KID Val resonance envelope [centered at about 0.90 ppm, 20.5 ppm (^{1}H, ^{13}C)].

Assignment of methyl resonances of Leu32 and Val36 within sub-domain D1. The resonances for some methyl groups in Leu and Val residues within the D1 and LH sub-domains can be identified by comparing the 2D [^{1}H,^{13}C] HMQC spectra of the p27-KID/Cdk2/cyclin A complex (Fig. S3E in the Supporting Material) with that for the sub-domain D2/Cdk2/cyclin A complex (Fig. S3D in the Supporting Material). The peaks that were absent in the spectrum of the sub-domain D2/Cdk2/cyclin A complex (Fig. S3D in the Supporting Material) can be assigned as being within the D1 and LH sub-domains of p27-KID [at 0.30 ppm, 25.4 ppm; and 0.16 ppm, 20.4 ppm (^{1}H, ^{13}C)]. These peaks appeared at essentially the same chemical shifts in the spectrum of the p27-KID/cyclin A complex, in which only sub-domain D1 was bound to cyclin A (Fig. S3B in the Supporting Material) (1, 10). These comparisons allowed assignment of one methyl group of Leu32 [at 0.30 ppm, 25.4 ppm (^{1}H, ^{13}C)] and one methyl group of Val36 [at 0.16 ppm, 20.4 ppm (^{1}H, ^{13}C)] (as noted in Fig. 4B).

Assignment of methyl resonances of Val79 and Leu70 or Leu84 (Leu70/84) within sub-domain D2. These two resonances were assigned by a process of elimination, as follows. Comparison of 2D [^{1}H,^{13}C] HMQC spectra for p27-KID/Cdk2/cyclin A and p27-KID/Cdk2 (Fig. S3E and C, respectively, in the Supporting Material) identifies two pair of resonances in the Leu region [at 0.98 ppm, 26.2 ppm; 0.88 ppm, 26.2 ppm; 0.95 ppm, 23.8 ppm; and 0.78 ppm, 22.4 ppm (^{1}H, ^{13}C)] present in the former spectrum that are absent in the latter. These resonances must arise from unassigned Leu residues within the LH or D1 sub-domains (Leu41 and Leu45) which do not directly bind to Cdk2. Furthermore, comparison of spectra for p27-KID/Cdk2/cyclin A and p27-KID^{LH3G}/Cdk2/cyclin A (Fig. S3E and H, respectively, in the Supporting Material) reveals that one pair of these resonances [at 0.98 ppm, 26.2 ppm; and 0.88 ppm, 26.2 ppm (^{1}H, ^{13}C)] is absent in the latter spectrum and present in the former; these are assigned to Leu41, which is mutated to Gly in the p27-KID^{LH3G} construct. The second pair of resonances [at 0.95 ppm, 23.8 ppm; and 0.78 ppm, 22.4 ppm (^{1}H, ^{13}C)] exhibits slight shifts in position but can be assigned to Leu45, which is present in the p27-KID^{LH3G} construct.

Comparison of 2D [^{1}H,^{13}C] HMQC spectra for p27-KID/Cdk2/cyclin A and p27-KID/Cdk2 (Fig. S3E and C, respectively, in the Supporting Material) identifies a resonance in the latter spectrum [at 0.78 ppm, 20.5 ppm (^{1}H, ^{13}C)] that arises from one (possibly both) both methyl group(s) of Val79 (the only unassigned Val residue).

Comparison of 2D [^{1}H,^{13}C] HMQC spectra for p27-KID/Cdk2/cyclin A and p27-KID/cyclin A (Fig. S3E and B, respectively, in the Supporting Material) identifies two pair of resonances in the Leu region [at 0.94 ppm, 25.1 ppm; 0.56 ppm, 25.4 ppm; 0.88 ppm, 22.2 ppm; and 0.70 ppm, 22.2 ppm (^{1}H, ^{13}C)] that are present in the former spectrum and are absent in the latter. Through a process of elimination, these resonances must arise from Leu70 and Leu84 within sub-domain D2 that binds Cdk2, but they cannot be specifically assigned. These ambiguous assignments are further confirmed by comparison of 2D [^{1}H,^{13}C] HMQC spectra for p27-KID/Cdk2/cyclin A and p27-KID/Cdk2 (Fig. S3E and C, respectively, in the Supporting Material) which shows that these same four resonances are present in both spectra.

Reported methyl resonance assignments. Through this process, we are confident about the assignments of many resonances. For simplicity, we have chosen to analyze only four assigned resonances in Figure 4B in the main text, those for one methyl each of Leu32 [at 0.30 ppm, 25.4 ppm (^{1}H, ^{13}C)], Val36 [at 0.16 ppm, 20.4 ppm (^{1}H, ^{13}C)], Leu70/84 [at 0.70 ppm, 22.24 ppm (^{1}H, ^{13}C)], and Val 79 [at 0.78 ppm, 20.5 ppm (^{1}H, ^{13}C)].

Kinase Activity/Inhibition Assays

A solution of 80 pM Cdk2/cyclin A, 2.5 μM histone H1 (Upstate, Charlottesville, VA) and varied concentrations of p27-KID^{wt} or the p27 sub-domain LH variants were incubated at 4 °C for 1 hour. ATP [total concentration, 100 μM; including 6 μCi γ^{32}P-ATP (Perkin Elmer, Waltham, MA)] was added to each reaction (15 μl total volume) and incubated at 30 °C for 35 minutes. Reactions were performed in kinase assay buffer containing 20 mM HEPES, pH 7.3, 25 mM sodium β-glycerolphosphate, 15 mM $MgCl_2$, 16 mM EGTA, 0.5 mM Na_3VO_4 and 10 mM DTT. Kinase reactions were quenched by adding SDS-PAGE gel loading buffer. Reaction products were analyzed by SDS-PAGE and ^{32}P-labeled Histone H1 bands were quantified using a Typhoon™ phosphoimager (GE Healthcare, Piscataway, NJ). The concentration dependence of p27-KID-, or p27-KID variant-, mediated inhibition of Cdk2-dependent phosphorylation of Histone H1 was fit to a dose-response model using Graphpad Prism software (Graphpad Software, Inc., San Diego, CA). The p27-KID (or p27-KID variant) concentration that caused 50% inhibition (IC_{50} values) was derived from the analysis of triplicate data sets and the errors are reported as the 95% confidence interval.

References

1. Lacy, E. R., I. Filippov, W. S. Lewis, S. Otieno, L. Xiao, S. Weiss, L. Hengst, and R. W. Kriwacki. 2004. p27 binds cyclin-CDK complexes through a sequential mechanism involving binding-induced protein folding. Nat. Struct. Mol. Biol. 11:358-364.
2. Hengst, L., V. Dulic, J. M. Slingerland, E. Lees, and S. I. Reed. 1994. A cell cycle-regulated inhibitor of cyclin-dependent kinases. Proc. Natl. Acad. Sci. USA 91:5291-5295.
3. Bowman, P., C. A. Galea, E. Lacy, and R. W. Kriwacki. 2006. Thermodynamic characterization of interactions between p27(Kip1) and activated and non-activated Cdk2: intrinsically unstructured proteins as thermodynamic tethers. Biochim Biophys Acta 1764:182-189. Epub 2006 Jan 2011.
4. Neidhardt, F. C., P. L. Bloch, and D. F. Smith. 1974. Culture medium for enterobacteria. J. Bact. 119:736-747.
5. Gill, S. C., and P. H. von Hippel. 1989. Calculation of protein extinction coefficients from amino acid sequence data. Anal Biochem 182:319-326.
6. Gasteiger, E., C. Hoogland, A. Gattiker, S. Duvaud, M. R. Wilkins, R. D. Appel, and A. Bairoch. 2005. Protein Identification and Analysis Tools on the ExPASy Server. In Proteomics Protocols Handbook. J. M. Walker, editor. Humana Press, Totowa, NJ
7. Delaglio, F., S. Grzesiek, G. W. Vuister, G. Zhu, J. Pfeifer, and A. Bax. 1995. NMR Pipe: A multidimensional spectral processing system based on UNIX pipes. J. Biomol. NMR 6:277-293.
8. Keller, R. 2004. The Computer Aided Resonance Assignment Tutorial. CANTINA Verlag and Rochus Keller.
9. Grimmler, M., Y. Wang, T. Mund, Z. Cilensek, E. M. Keidel, M. B. Waddell, H. Jakel, M. Kullmann, R. W. Kriwacki, and L. Hengst. 2007. Cdk-inhibitory activity and stability of p27Kip1 are directly regulated by oncogenic tyrosine kinases. Cell 128:269-280.
10. Russo, A. A., P. D. Jeffrey, A. K. Patten, J. Massague, and N. P. Pavletich. 1996. Crystal structure of the p27Kip1 cyclin-dependent-kinase inhibitor bound to the cyclin A-Cdk2 complex. Nature 382:325-331.

Supporting Figure Legends

Figure 1 (A) Crystal structure of the p27/Cdk2/Cyclin A complex (PDB ID: 1JSU). p27, Cdk2, and Cyclin A are colored red, blue, and green respectively. NMR data for the p27 residues indicated as yellow spheres (C29, R30, N311, L32, V36, G72, E75, Q77, Y88, V79, and L84) are illustrated in Fig. 5. **(B)** An expanded view of the boxed region in **(A)** showing a network of electrostatic interactions between residues within the p27 LH sub-domain and the interaction of L41 of p27 with Cyclin A.

Figure S2 [^{1}H,^{15}N] TROSY spectra of **(A)** unbound p27-KID^{wt}, **(B)** p27-KID^{wt} bound to cyclin A, **(C)** p27-KID^{wt} bound to Cdk2, **(D)** p27-KID^{D2} bound to Cdk2/Cyclin A, **(e)** p27-KID^{wt} bound to Cdk2/Cyclin A, **(F)** p27-KID^{p21LH} bound to Cdk2/Cyclin A, **(G)** p27-KID^{p57LH} bound to Cdk2/Cyclin A, and **(H)** p27-KID^{LH3G} bound to Cdk2/Cyclin A. All p27 constructs were U-^{2}H/^{15}N, ILV-^{1}H/^{13}C-methyl-labeled and Cdk2 and cyclin A were unlabeled.

Figure S3 [^{1}H,^{13}C] HMQC spectra of **(A)** unbound p27-KID^{wt}, **(B)** p27-KID^{wt} bound to cyclin A, **(C)** p27-KID^{wt} bound to Cdk2, **(D)** p27-KID^{D2} bound to Cdk2/Cyclin A, **(E)** p27-KID^{wt} bound to Cdk2/Cyclin A, **(F)** p27-KID^{p21LH} bound to Cdk2/Cyclin A, **(G)** p27-KID^{p57LH} bound to Cdk2/Cyclin A, and **(H)** p27-KID^{LH3G} bound to Cdk2/Cyclin A. All p27 constructs were U-^{2}H/^{15}N, ILV-^{1}H/^{13}C-methyl-labeled and Cdk2 and cyclin A were unlabeled.

Figure S4 Thermal denaturation curves for complexes of p27-KID^{wt}, p27-KID^{p21LH}, p27-KID^{p57LH} or p27-KID^{LH3G} bound to Cdk2/cyclin A. CD ellipticity at 222 nm for solutions containing each complex at 400 nM was recorded with heating with constant stirring from 15 ˚C to 95 ˚C. The change in ellipticity at 222 nM was used to monitor the unfolding process. Thermal denaturation curves for ternary complexes containing p27-KID^{wt}, p27-KID^{p21LH}, p27-KID^{p57LH} and p27-KID^{LH3G} are colored red, green, blue, and purple, respectively.

Figure S5 Raw data for Cdk2/cyclin A inhibition assays. Autoradiography analysis of SDS-PAGE results of phosphorylation of Histone H1 (PO_4-H1) by Cdk2/cyclin A in the presence of increasing concentrations of p27-KID^{wt}, the other LH sub-domain variants, or sub-domain D2.

Supplementary Figures

Figure S1

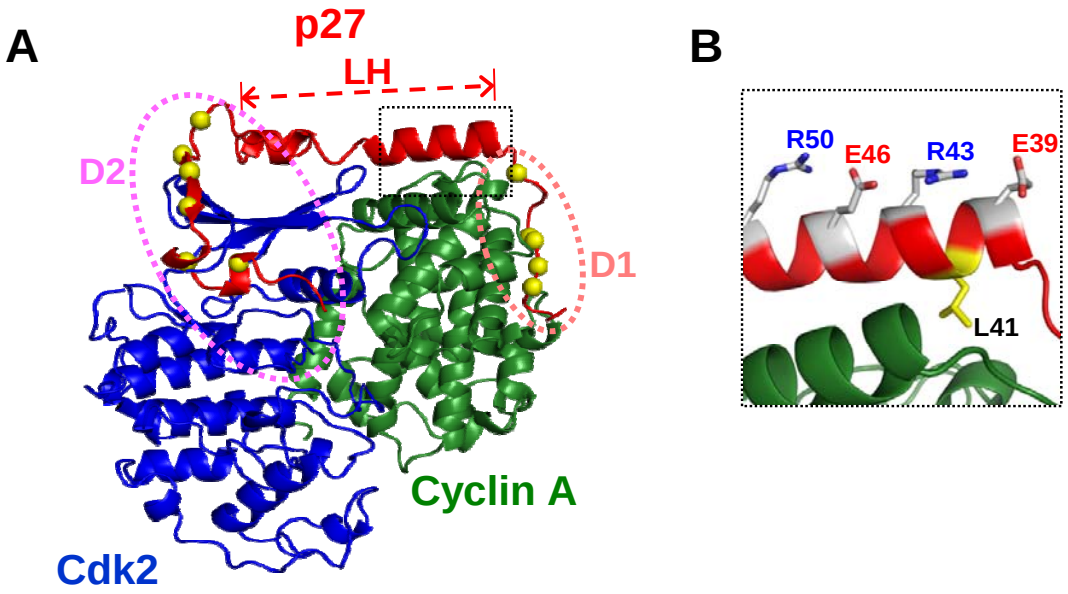

Figure S2

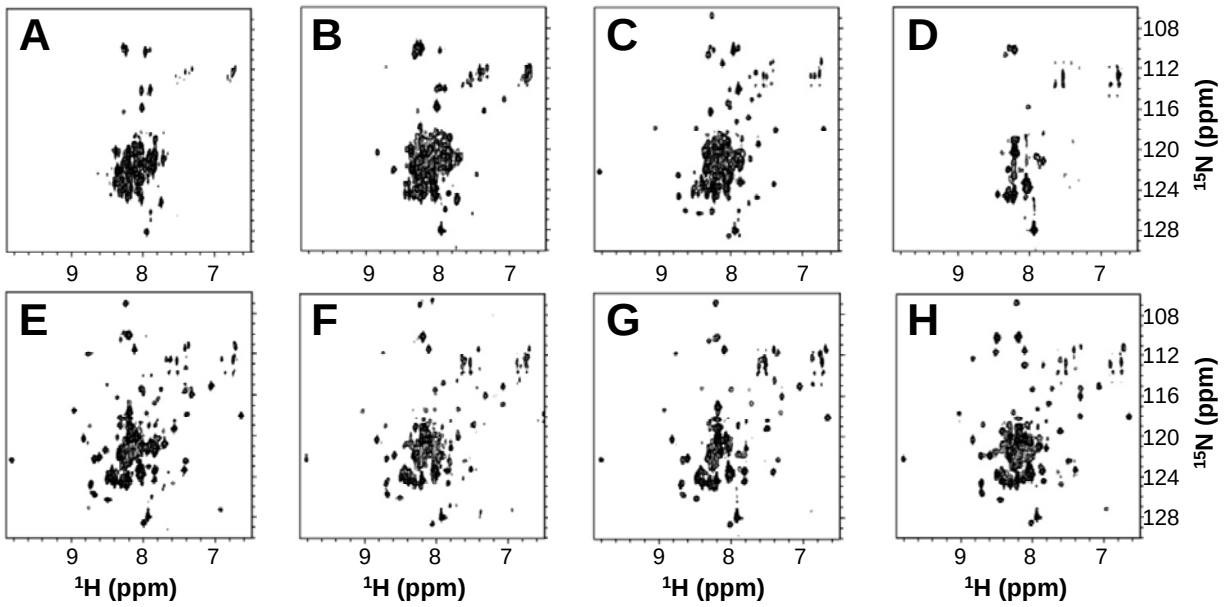

Figure S3

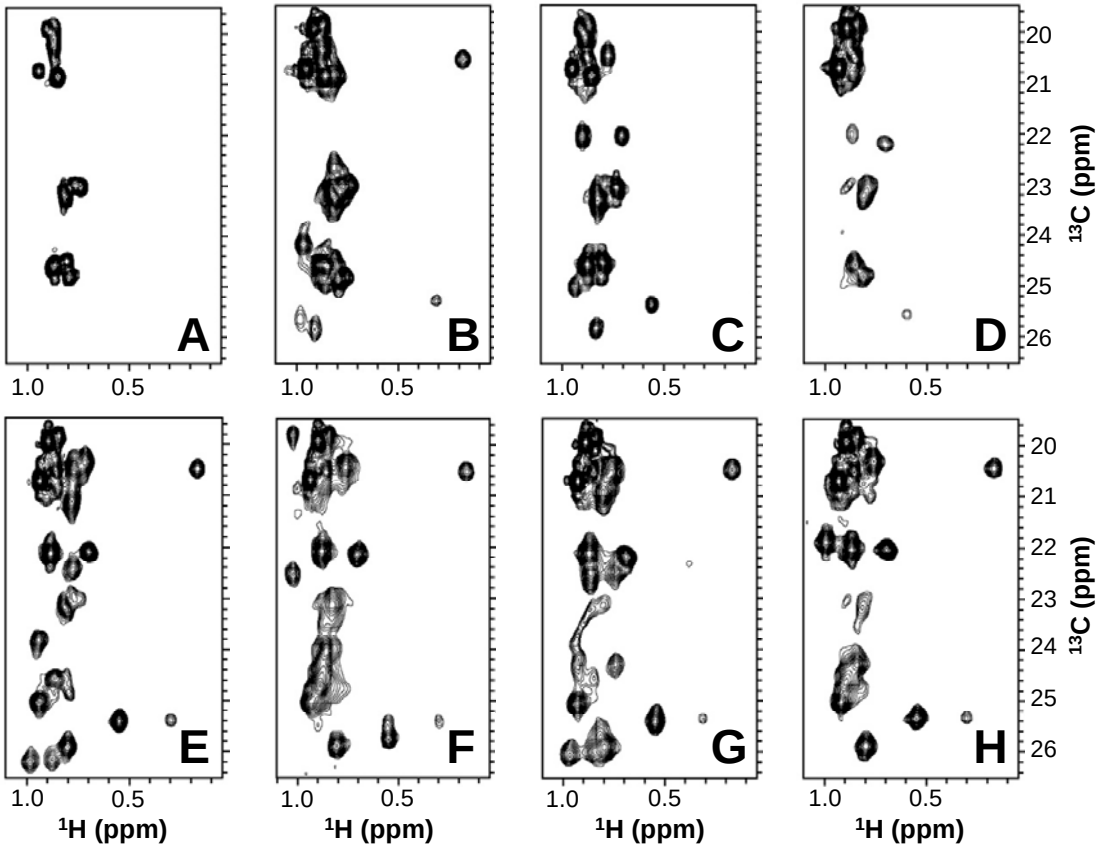

Figure S4

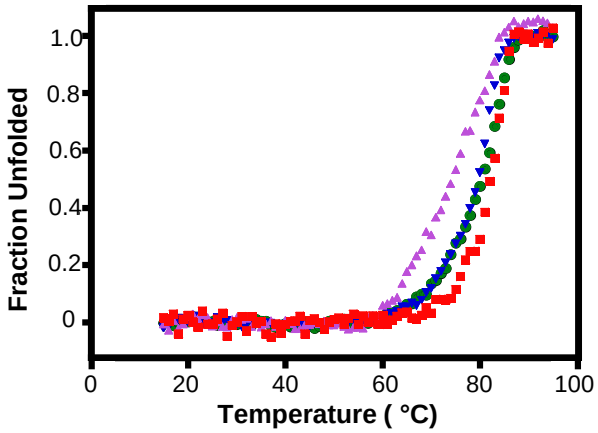
Fraction Unfolded
1.0
0.8
0.6
0.4
0.2
0
0
20
40
60
80
100
Temperature (°C)

Figure S5

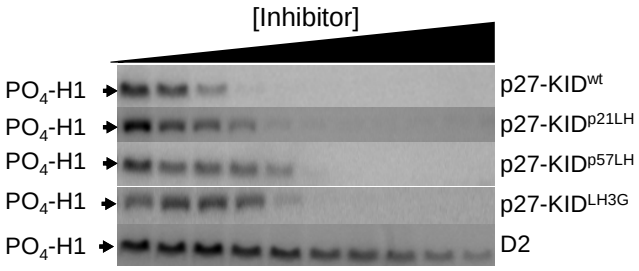
[Inhibitor]
PO4-H1
p27-KIDwt
PO4-H1
p27-KIDp21LH
PO4-H1
p27-KIDp57LH
PO4-H1
p27-KIDLH3G
PO4-H1
D2